CrystEngComm

Cite this: *CrystEngComm*, 2012, **14**, 7686–7693

www.rsc.org/crystengcomm

PAPER

Microwave-assisted route to fabricate coaxial ZnO/C/CdS nanocables with enhanced visible light-driven photocatalytic activity†

Mojiao Zhou, Yong Hu,* Yu Liu, Wenlong Yang and Haisheng Qian

Received 11th April 2012, Accepted 31st May 2012
DOI: 10.1039/c2ce25540e

In this work, novel one-dimensional (1D) coaxial nanostructures composed of ZnO nanorod cores, intermediate amorphous carbonaceous layers, and CdS nanoparticle sheaths (*i.e.* ZnO/C/CdS nanocables) have been successfully synthesized *via* a multi-step process. First, ZnO/C core-shell nanocables are assembled *via* a facile hydrothermal reaction of ZnO nanorods and glucose in water at 160 °C for 6 h. Second, CdS nanoparticles are uniformly anchored on the surface of the ZnO/C core-shell nanocables through a rapid microwave irradiation route to form ternary coaxial ZnO/C/CdS nanocables. Further investigation reveals that the thickness of carbonaceous layer and the amount of CdS nanoparticles can be regulated by controlling of the glucose intake and the cadmium salt concentration, respectively. Due to stronger adsorption, and the synergistic effect of the ternary ZnO/C/CdS interface, the as-prepared nanohybrids exhibit an exceptionally higher activity than that of pure ZnO nanorods, pure CdS and ZnO/C core-shell nanocables for the degradation of rhodamine-B (RhB) and methylene blue (MB) under visible-light irradiation. The result also indicates that controlling the thickness of the carbonaceous layer and the amount of CdS nanoparticles in coaxial ZnO/C/CdS nanocables are crucial to obtaining an optimal synergistic effect between the three of them. Furthermore, it is believed that this facile strategy is scalable and its application can be extended to synthesize other 1D coaxial ternary nanocables for different applications.

Introduction

The trace amount of toxic organic compounds, such as dyes and polymer additives, in-water bodies and waste-water, will pose severe environmental pollution and health problems.[1] Under unremitting efforts, people have explored several appropriate ways to eliminate these contaminants, for example, coagulation, acid out, biochemical process, liquid membrane separation and granular activated carbon method, *etc.*[2,3] As a kind of non-biological technology to degrade the dye pollutants and which won't pollute water the second time, photocatalysis has received an enormous amount of research interest.[4,5] Metal oxide photocatalysts, such as TiO_2 or ZnO, are promising materials that possess the characteristics of energy-saving, green, environmental-protecting and high-efficiency by utilizing solar and/or UV light.[6,7]

As one of the most important multifunctional semiconductor materials, ZnO has a wide-band gap (E_g = 3.37 eV) and large excitation binding energy (E_B = 60 meV).[8] ZnO appears to be a suitable alternative to TiO_2 since its photodegradation mechanism has been proven to be similar to that of TiO_2.[9] Furthermore, ZnO synthetic methods are simple, low-temperature, non-toxic, environmentally-friendly, and possess an enormous potential for commercialization.[10] Specially, one-dimensional (1D) ZnO nanorods (NRs) have been extensively studied as photocatalysts for their large length–diameter ratio, high specific strength and high ratio surface area.[11,12]

However, the photo-corrosion of ZnO that occurs with the UV light irradiation, as well as the susceptibility of ZnO to facile dissolution at extreme pH values, have significantly decreased the photocatalytic activity of ZnO in aqueous solution and blocked the application of ZnO in photocatalysis.[13] To overcome these obstacles, it is often necessary to coat the ZnO NRs surface with an amorphous carbon shell.[14] Additionally, new functionalities might also be introduced into the coatings, such as optical properties, catalytic or absorbing capacity.[15] Amorphous carbon, which can be obtained *via* inexpensive and environmentally benign hydrothermal processes using glucose as a precursor, is an interesting and unique coating material for nanostructures.[16–20] The surface of the amorphous carbon is hydrophilic and has an abundant amount of –OH and $–COO^-$ groups. When dispersed in metal salt solutions, these surface functional groups can bind metal cations through coordination or electrostatic interactions. In addition, there are nanosized pores distributed uniformly on the surface of the carbon coatings. These pores could not only

Key Laboratory of the Ministry of Education for Advanced Catalysis Materials, Institute of Physical Chemistry, Zhejiang Normal University, Jinhua, 321004, P. R. China. E-mail: yonghu@zjnu.edu.cn
† Electronic supplementary information (ESI) available. See DOI: 10.1039/c2ce25540e

increase the surface area, but also facilitate penetration of reactive species.[21,22]

Cadmium sulfide (CdS) is a very important II–VI semiconductor, which can absorb most of the solar spectrum with a direct band gap energy of 2.42 eV.[23] Recently, CdS nanoparticle based photocatalysts for the degradation of dyes in wastewater under visible light irradiation have attracted intense interest, in view of their unique photochemical and photophysical properties.[24,25] To reduce the aggregation and enhance the visible-light-driven activity, we have previously employed loading of CdS nanoparticles on the surface of colloidal carbon spheres and observed significantly enhanced photocatalytic activity.[26,27]

To further improve the photocatalytic activity, we have designed a unique ternary photocatalyst based on 1D ternary coaxial ZnO/C/CdS nanocables *via* a hydrothermal process and a microwave-assisted deposition method in this work (Scheme 1). First, ZnO/C core-shell nanocables are obtained by a facile hydrothermal reaction of pre-formed ZnO NRs and glucose in water. The thickness of the amorphous carbonaceous layer can be varied by the amount of glucose. Second, CdS nanoparticles are anchored on the surface of ZnO/C core-shell nanocables to form ternary coaxial ZnO/C/CdS nanocables *via* a rapid microwave-assisted method, which has the advantages of leading to a small particle size, narrow particle size distribution, and high purity in comparison to the conventional methods.[28–32] Here, the amount and size of the CdS nanoparticles is conveniently controlled by varying the concentration of metal salt precursor. In such hybrid structures, in addition to all the desired functions of each constituent, some strong synergetic effects can be achieved by integrating the individual components, hence realizing the full potential of the nanocomposite materials. By combining ZnO NRs, carbon, with CdS nanoparticles, one might be able to take advantage of all these components. As expected, the as-prepared ternary photocatalysts exhibit excellent synergistic effects for the degradation of dyes (RhB and MB) when exposed to visible-light irradiation. These nanohybrids exhibit an exceptionally higher activity than that of pure ZnO NRs, pure CdS and ZnO/C core-shell nanocables. Moreover, the result also clearly indicates that controlling the thickness of carbon layer and the amount of CdS nanoparticles in coaxial ZnO/C/CdS nanocables is crucial to obtain an optimal synergistic effect between the three of them.

Experimental

All reagents were of analytical grade, purchased from the Shanghai Chemical Reagent Manufacturing Co., and used as received without further purification.

Synthesis of ZnO NRs

In a typical procedure, 16 mL of 0.1 M zinc acetate ($Zn(Ac)_2{\cdot}2H_2O$) stock solution in ethanol was mixed with 32 mL of 0.5 M NaOH solution in ethanol to obtain a clear solution. Then, the resulting mixture was transferred to a 60 mL Teflon-lined stainless steel autoclave and heated at 150 °C for 12 h.[33] Finally, the white ZnO NRs were washed repeatedly with distilled water and ethanol for several times, and then dried in an oven at 60 °C for 6 h.

Synthesis of ZnO/C core-shell nanocables

In a typical experiment, 0.05 g of ZnO NRs and a certain amount of glucose were added into 16 mL of distilled water and were well dispersed with the assistance of ultrasonication for 10 min. The mixture was sealed into a 20 mL of Teflon-lined stainless steel autoclave and maintained at 160 °C for 6 h.[34] After it was cooled down to room temperature, the brown products were collected and washed by distilled water and ethanol several times, and dried in an oven at 60 °C for 6 h. Products prepared with different amounts of glucose (0.1 g, 0.2 g, and 0.3 g) after the hydrothermal process were named as H-0.1, H-0.2 and H-0.3.

Synthesis of ternary coaxial ZnO/C/CdS nanocables

In a typical procedure, a certain amount of $CdCl_2{\cdot}2H_2O$ was added into a round-bottom flask and dissolved in a solvent containing 10 mL of ethanol and 10 mL of distilled water, which formed a clear solution. A 0.05 g portion of the as-prepared ZnO/C core-shell nanocables was added into the above solution and was well dispersed with the assistance of ultrasonication for 10 min. Then, the Cd^{2+}-ZnO/C core-shell nanocable solution was stirred and maintained at 60 °C for 6 h to arrive at the saturated extent of adsorption and then was collected by centrifugation. To remove possible superfluous cations and anions, the obtained products were washed with ethanol and distilled water three times. The above-obtained samples and 0.02 g of thioacetamide (TAA) were placed in a microwave refluxing system (MCR-3, Shanghai Puredu BIO-TECH Co., Ltd.) with a controlled power of 280 W and reacted at 150 °C for 10 min under atmospheric pressure, resulting in ternary coaxial ZnO/C/CdS nanocables. After being cooled to ambient temperature, the final products were collected and washed with ethanol and distilled water three times before drying at 60 °C for 6 h. To investigate the effect of Cd-absorbed on the formation of coaxial ZnO/C/CdS nanocables, the different concentration of $CdCl_2{\cdot}2H_2O$ was used in the adsorption process, while the other conditions remain unchanged. Products prepared with different concentrations of $CdCl_2{\cdot}2H_2O$ (0.0035, 0.0070, 0.0140, 0.0210 and 0.0280 M) after

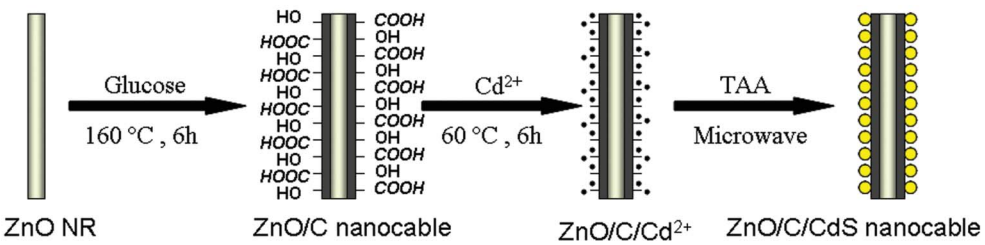

Scheme 1 Schematic illustration of the formation of ternary coaxial ZnO/C/CdS nanocables.

Table 1 Control of CdS particle size in coaxial ZnO/C/CdS nanocables using different Cd^{2+} concentration

Sample	Cd^{2+} concentration/M	CdS particle size/nm[a]
Sa	0.0035	2.4
Sb	0.0070	3.9
Sc	0.0140	5.5
Sd	0.0210	7.8
Se	0.0280	9.3

[a] CdS particle size was calculated from XRD diffraction data.

the microwave irradiation routes were assigned sample codes Sa, Sb, Sc, Sd and Se, respectively (see Table 1).

Characterization

Powder X-ray diffraction (XRD) measurements of the samples were performed with a Philips PW3040/60 X-ray diffractometer using Cu-Kα radiation at a scanning rate of $0.06^\circ\ s^{-1}$. Scanning electron microscopy (SEM) was performed with a Hitachi S-4800 scanning electron microanalyzer with an accelerating voltage of 15 kV. Transmission electron microscopy (TEM) and high-resolution transmission electron microscopy (HRTEM) were conducted at 200 kV with a JEM-2100F field emission TEM. Energy dispersive X-ray spectrometry (EDS) was performed with a spectroscope attached to HRTEM. Samples for TEM measurements were prepared by dispersing the products in ethanol and placing several drops of the suspension on holey carbon films supported by copper grids. The absorption spectra were measured using a PerkinElmer Lambda 900 UV-vis spectrophotometer at room temperature.

Photocatalytic activity of ternary coaxial ZnO/C/CdS nanocables

Photocatalytic activities of the as-prepared coaxial ZnO/C/CdS nanocables were evaluated by the degradation of RhB and MB under visible-light irradiation of a 500 W Xe lamp (CEL-HXF300) with a 420 nm cut off filter. The reaction cell was placed in a sealed black box with the top opened, and the cut off filter was placed to provide visible-light irradiation. In a typical process, 0.04 g of as-prepared photocatalysts were added into 100 mL of RhB solution (concentration: 5 mg L^{-1}) and MB solution (concentration: 10 mg L^{-1}), respectively. After being dispersed in an ultrasonic bath for 5 min, the solution was stirred for 2 h in the dark to reach adsorption equilibrium between the catalyst and the solution and then was exposed to visible-light irradiation. The samples were collected by centrifugation at given time intervals to measure the dyes degradation concentration by UV-vis spectroscopy.

Results and discussion

The excess glucose during the hydrothermal process will lead to excessive carbon, thus causing the ZnO NRs to become coated with a thick and dense carbon layer, which can prevent the inherent optical absorption of ZnO and result in the rapid decrease of the quantity of photogenerated charges, and finally reduce the photocatalytic activity.[34] To choose an appropriate thickness of the carbon layer for the loading CdS nanoparticles, we used different amounts of glucose in our experiments. Fig. 1a shows the XRD patterns of the as-prepared pure ZnO NRs and ZnO/C core-shell nanocables with different amounts of glucose. For pure ZnO NRs, all the diffraction peaks can be indexed as the wurtzite phase of ZnO with lattice constants of a = 3.250 Å and c = 5.207 Å, which is consistent with the standard XRD data file of ZnO (JCPDS standard card no. 79-2205). No impurity peaks are detected showing that the products are pure phase. For the as-prepared ZnO/C core-shell nanocables obtained with the different amounts of glucose, all the diffraction peaks also illustrate that all samples are pure ZnO. Thus, glucose used in the hydrothermal synthesis does not affect the crystalline phase of ZnO. But the peak intensity weakened with the glucose addition, indicating the amorphous carbon layer can cause scattering of the X-rays.[14]

The photocatalytic activity of different samples was evaluated by the degradation of RhB dye after exposure to visible light irradiation. Fig. 1b displays the photodegradation behaviour of RhB catalyzed by a blank, the as-prepared pure ZnO NRs and coaxial ZnO/C core-shell nanocables obtained with the different amounts of glucose, where C is the concentration of RhB after different light irradiation times and C_0 is the initial concentration of the RhB before dark adsorption. After stirring for 2 h in the dark, the adsorption capacity of RhB using different samples (pure ZnO NRs, H-0.1, H-0.2, and H-0.3) as adsorbents are about 8.8, 15.1, 19.0 and 22.4%, respectively. However, samples H-0.2, and H-0.3 exhibit enhanced photoactivity for RhB degradation as compared to pure ZnO NRs, and H-0.2 shows the best photodegradation activity. After visible light irradiation for 60 min, the de-colorization fractions using different samples (pure ZnO NRs, H-0.1, H-0.2, and H-0.3) as photocatalysts are about 32.4, 51.3, 58.3, and 46.3%, respectively. This result indicates the as-prepared ZnO/C core-shell nanocable photocatalysts are only slightly more active than pure ZnO NRs. The enhanced degradation efficiency of the as-prepared ZnO/C core-shell nanocables may be ascribed to the synergy effect of carbon and ZnO. First, amorphous carbons possess superior adsorption ability, and hence RhB can be enriched on the surface of photoactive ZnO, resulting in the acceleration of the rate of photocatalytic reaction. Second, the coating of amorphous carbon improves the absorption of ZnO toward visible light, which means that more photons can be absorbed and be utilized for the photocatalytic reaction. However, the thick and dense carbon layer can prevent the inherent optical absorption of ZnO and result in the decrease of the photocatalytic activity. Thus, there is an optimal thickness of amorphous carbonaceous layer for photocatalysis. In our work, the best photocatalytic activity of sample H-0.2 was used in our further experiments.

Fig. 2 shows the XRD patterns of ternary coaxial ZnO/C/CdS nanocables using sample H-0.2 as the template by adding different concentrations of Cd^{2+} and the same concentration of TAA *via* a microwave-assisted method. From these patterns, they obviously consist of two sets of diffraction peaks (ZnO and CdS); the broadened diffraction peaks at 2θ values of 26.8°, 44.0° and 52.1° match well with the crystal planes of the (111), (220), and (311) of face-centered cubic (fcc) CdS (JCPDS standard card no.75-0581, a = 5.810 Å). With the increase of Cd^{2+} concentration, the diffraction intensity of the CdS (111) crystal plane becomes gradually stronger, indicating the CdS nanoparticles grow gradually larger and larger. In addition, the average size of CdS nanoparticles as the concentration of Cd^{2+} increases,

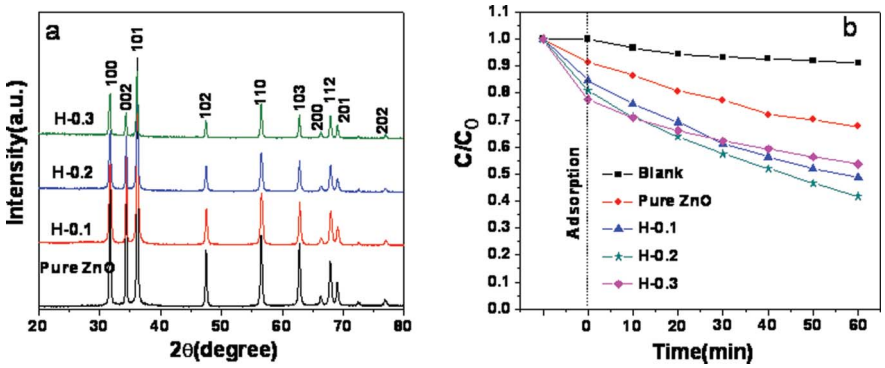

Fig. 1 (a) XRD patterns of the as-prepared pure ZnO NRs and 1D ZnO/C core-shell nanocables obtained with different amounts of glucose. (b) Photocatalytic degradation of RhB in the presence of the as-prepared pure ZnO NRs and the ZnO/C core-shell nanocables obtained with different amounts of glucose: sample H-0.1, H-0.2 and H-0.3.

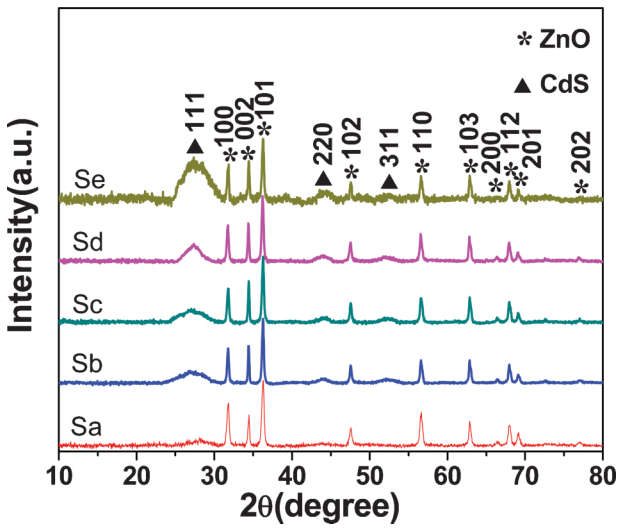

Fig. 2 XRD patterns of the as-prepared 1D coaxial ZnO/C/CdS nanocables obtained with different concentrations of Cd^{2+} *via* a microwave-assisted method.

calculated using the Debye–Scherrer equation based on the full width at half-maximum of the diffraction peak, are 2.4, 3.9, 5.5, 7.8 and 9.3 nm, respectively (see Table 1).

The SEM images of the as-prepared ZnO/C core-shell nanocables (sample H-0.2) and ternary coaxial ZnO/C/CdS nanocables obtained using different concentrations of Cd^{2+} are shown in Fig. 3. From Fig. 3a, the size of the as-prepared ZnO/C core-shell nanocables is about 80 nm in diameter and a range of 0.5–2 μm in length. Furthermore, no by-products such as carbon spheres or particles were seen during SEM observations, which indicated that the carbonization occurred accurately on the surface of the ZnO NRs. As seen from Fig. 3b–f, obvious morphological changes can be observed. With increasing concentrations of Cd^{2+}, the surface of the ZnO/C core-shell nanocables became rougher and thicker, indicating the size of CdS nanoparticles increased gradually. For comparison, the SEM images of the as-prepared pure ZnO NRs and ZnO/C core-shell nanocables obtained with the different amounts of glucose are shown in Fig. S1, ESI.† It is obvious that the ZnO/C core-shell nanocables became thicker as the glucose concentration increased.

Further morphology and structure characterizations of the as-prepared samples are shown in Fig. 4. Fig. 4a is a TEM image of a single coaxial ZnO/C/CdS nanocable, which clearly shows ZnO NR is encapsulated by an amorphous carbonaceous layer and CdS nanoparticles are uniformly deposited on the surface of the carbon layer. The rough surface may provide a higher specific area and be beneficial for the photocatalytic degradation of organic pollutants. From the HRTEM image (inset in Fig. 4a), it can be clearly seen that the thickness of the amorphous carbonaceous layer is about 5 nm and the size of CdS nanoparticles is about 5.5 nm. The fringe spacing of ZnO NR is about 0.52 nm, which is close to the separation between the (0001) lattice planes. Thus, the axial direction of the as-prepared ZnO NRs is perpendicular to the normal direction of the (0001) lattice plane of the hexagonal ZnO.[35] For comparison, the HRTEM images of the as-prepared coaxial ZnO/C/CdS nanocables obtained with the different amounts of glucose are shown in Fig. S2, ESI.† From these images, it can be seen that the thickness of the amorphous carbonaceous layer could be easily tuned by controlling the amount of glucose. The carbon layer thickness changes from 3 to 10 nm while the glucose amount is increased from 0.1 to 0.3 g in this work. Fig. 4b shows the as-prepared coaxial ZnO/C/CdS nanocables using the higher concentration of Cd^{2+} (sample Se); it can be found that more CdS nanoparticles are anchored onto the amorphous carbonaceous layer. The HRTEM image of the sample (inset in Fig. 4b) reveals the size of the CdS nanoparticles become larger with the increasing of the Cd^{2+} concentration, which is in accord with that of the XRD data. The EDS pattern (inset in Fig. 4b) on the obtained coaxial ZnO/C/CdS nanocables reveals the existence of Zn, Cd, C, O and S elements, further confirming the formation of CdS species on the surface of ZnO/C core-shell nanocables. The uniform amorphous carbonaceous layers possibly formed by the carbonization of glucose around the ZnO NRs involving the intermolecular cross-linking and dehydration of the glucose molecules, oligosaccharides, and/or other macromolecules derived from glucose during the hydrothermal treatment.[22] This carbonaceous layer with hydrophilic functional groups is very helpful to facilitate the dispersion of the nanostructures by preventing them from aggregation in aqueous solutions. Meanwhile, the hydrophilic groups can serve as anchors to immobilize Cd^{2+} ions on the carbon layer surface.[21] Thus, the

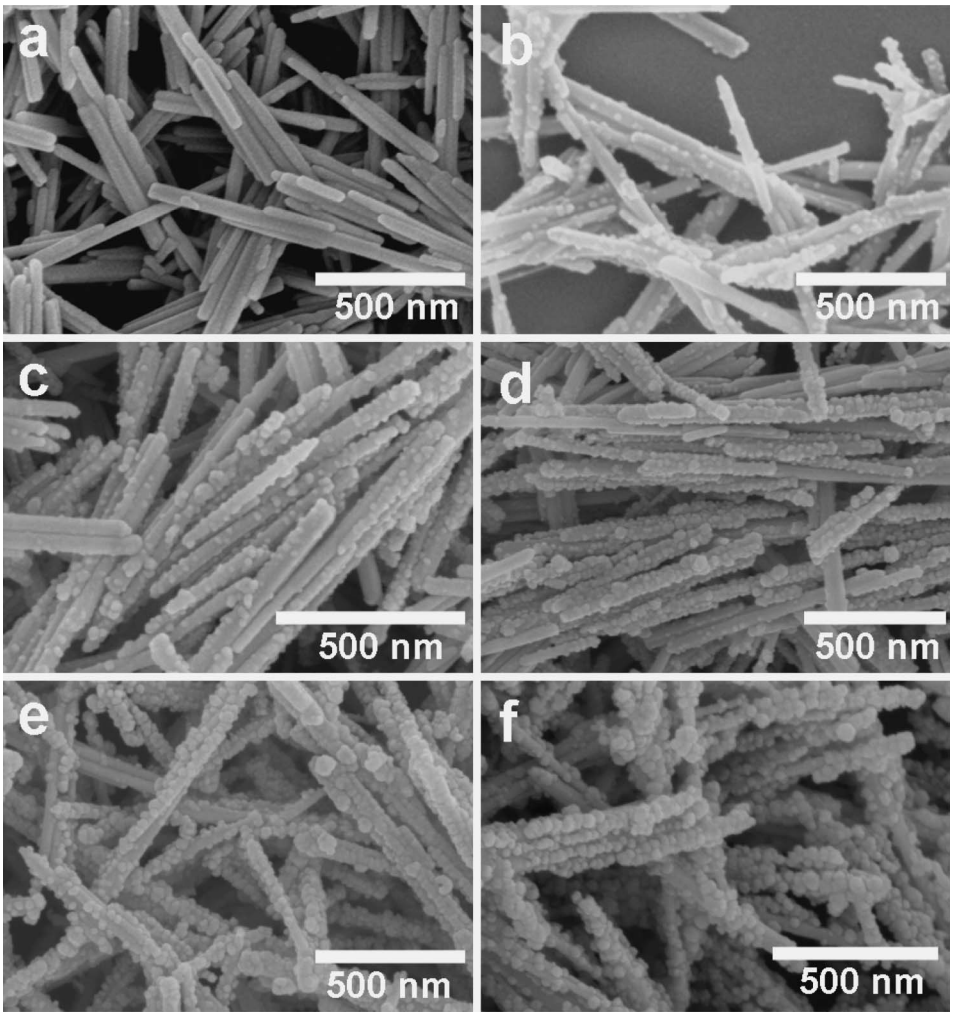

Fig. 3 SEM images of the as-prepared ZnO/C core-shell nanocables using 0.2 g of glucose (a), and ternary coaxial ZnO/C/CdS nanocables obtained with the different Cd^{2+} concentrations: (b) 0.0035 M, (c) 0.0070 M, (d) 0.0140 M, (e) 0.0210 M, and (f) 0.0280 M.

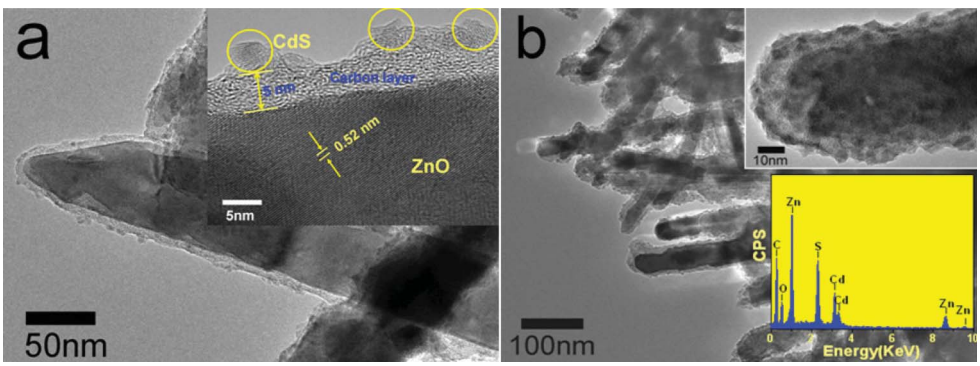

Fig. 4 TEM images of the as-prepared ternary coaxial ZnO/C/CdS nanocables using (a) 0.0140 M of Cd^{2+} (inset: HRTEM image), and (b) 0.0280 M of Cd^{2+} (inset: HRTEM image and EDS pattern).

carbonaceous layer with bound hydrophilic groups inherited from the starting materials acted as both the linker and the stabilizer between ZnO and CdS.[36]

Fig. 5a displays the photodegradation behaviour of RhB dye in the presence of the as-prepared ternary coaxial ZnO/C/CdS nanocable photocatalysts obtained with the different concentrations of Cd^{2+} after exposure to visible light irradiation. It can be seen that when the concentration of Cd^{2+} was less than 0.0140 M, the photoactivity was enhanced steadily with increasing concentrations of Cd^{2+}. However, further increases in the concentration of Cd^{2+} (>0.0140 M) during the microwave synthesis results in decreasing photocatalytic activity. The thicker and denser CdS layer may have reduced the quantity of the photogenerated charges due to the unfavorable morphology and also poorer

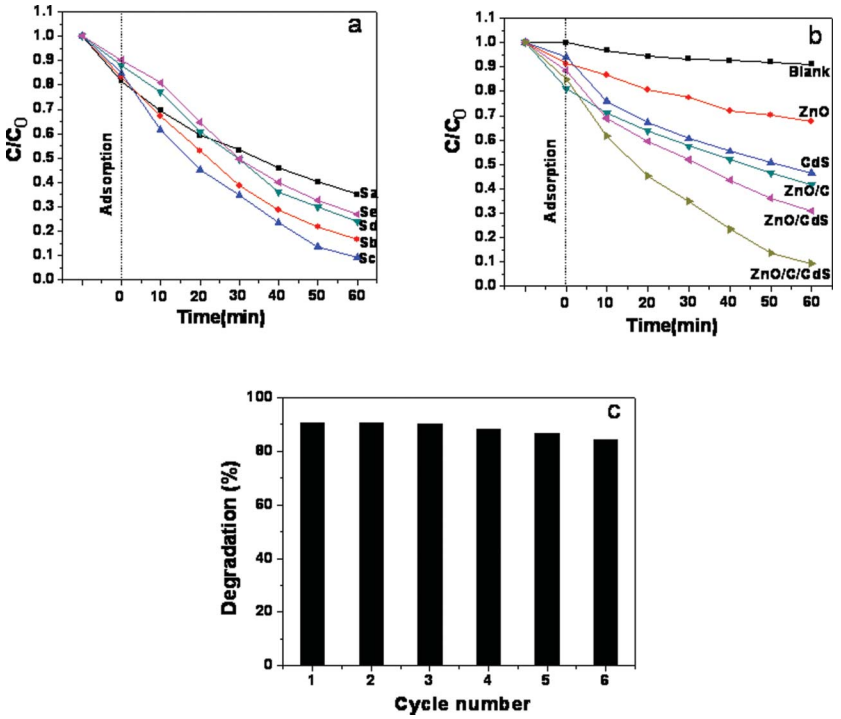

Fig. 5 (a) Photocatalytic degradation of RhB in the presence of the as-prepared ternary coaxial ZnO/C/CdS nanocables obtained with the different concentration of Cd^{2+}; (b) The photocatalytic activities in the absence of any photocatalyst (the blank test) and using different photocatalysts: pure ZnO NRs, pure CdS, H-0.2, ZnO/CdS binary composites and Sc. (c) 6 cycles of the degradation of RhB using sample Sc as a photocatalyst under visible light irradiation for 60 min.

charge transport through the CdS shell. The best degradation activity for RhB is attained in sample Sc, which indicates that the structure of sample Sc should have the ideal ZnO/C/CdS nanocable structure when the balancing of charge separation and transport is optimal and hence demonstrates the most favorable photocatalytic activity. Thus, we can conclude that there are two important roles in the nanocomposite of ZnO/C/CdS nanocables. One is the thickness of the amorphous carbonaceous layer, and the other is the amount of CdS nanoparticles. These two aspects together can explain why sample Sc with an appropriate composition exhibits the best photocatalytic activity. For comparison, the curves of the photodegradation efficiency with the irradiation time in the absence of any photocatalyst (the blank test) and in the presence of different photocatalysts, *i.e.* the pure ZnO NRs, pure CdS, sample H-0.2, and sample Sc, are shown in Fig. 5b. After visible-light irradiation for 60 min, 32.4% of RhB is degraded in the presence of pure ZnO NRs, while approximately 58.3% of RhB is decomposed using ZnO/C core-shell nanocables (sample H-0.2) as the photocatalyst. This indicates that this ZnO/C core-shell nanocable photocatalyst is only slightly more active than pure ZnO NRs. However, about 90.7% of RhB is degraded in the presence of the ternary coaxial ZnO/C/CdS nanocables (sample Sc) after only 60 min. Due to the highly synergistic effect of these ternary nanohybrids, the as-prepared fabricated functional nanostructures demonstrate a significantly higher photocatalytic activity than that of ZnO/C core-shell nanocables and CdS nanoparticles. Additionally, the ZnO/CdS binary composite was also prepared by a microwave-assisted reaction of the CdS precursor (the concentration of Cd^{2+} was 0.0140 M) and ZnO NRs for comparison. It shows only about 69.2% of RhB is degraded, which further confirms that the carbon can work as an active component. Furthermore, 1D nanostructures possess several advantageous features, such as a very high surface-to-volume ratio, enhanced light scattering and absorption, rapid transport of free electrons along the long direction and efficient electron-hole utilization (high quantum efficiency)[37] which results in the enhanced photocatalytic efficiency. The reusability of sample Sc as a photocatalyst is also investigated by collecting and reusing the same photocatalyst for multiple cycles. As shown in Fig. 5c, when sample Sc is used for the reusability test, the photocatalytic activity does not show significant loss for up to 6 cycles of photodegradation of RhB, indicating the stability of the ternary coaxial ZnO/C/CdS nanocables. Fig. 6 shows the photodegradation behaviors of MB, which exhibits a similar regularity like degrading RhB. This result further demonstrates that sample Sc possesses the optimal synergistic effect in the degradation of dyes under visible-light irradiation.

Conclusions

In summary, we have demonstrated the synthesis of a unique ternary photocatalyst based on 1D coaxial ZnO/C/CdS nanocables *via* a facile hydrothermal process and a rapid microwave-assisted deposition method. The thickness of the amorphous carbonaceous layer can be varied by the amount of glucose and the amount of CdS nanoparticles anchored is conveniently controlled by varying the concentration of the metal salt precursor. The fabricated functional nanohybrids demonstrated a significantly enhanced photocatalytic activity than that of pure ZnO nanorods, pure CdS, ZnO/CdS binary composites and

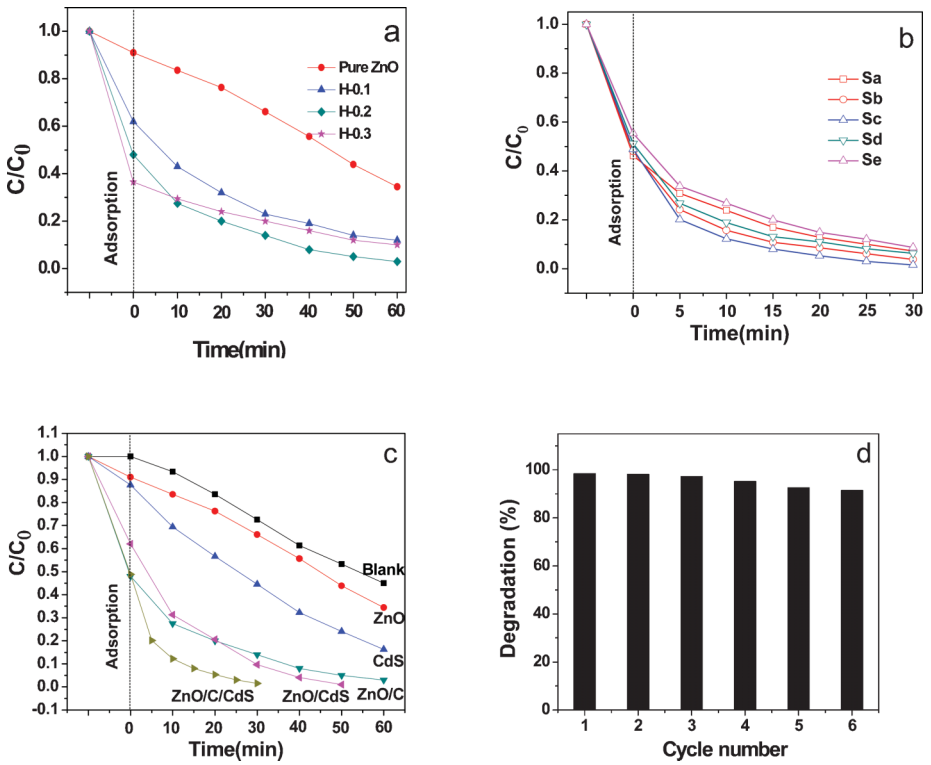

Fig. 6 (a) Photocatalytic degradation of MB in the presence of the as-prepared pure ZnO NRs and the ZnO/C core-shell nanocables obtained with the different amount of glucose: sample H-0.1, H-0.2 and H-0.3; (b) Photocatalytic degradation of MB in the presence of the as-prepared ternary coaxial ZnO/C/CdS nanocables obtained with the different concentrations of Cd^{2+}; (c) The photocatalytic activities in the blank test and using different photocatalysts: pure ZnO NRs, pure CdS, H-0.2, ZnO/CdS binary composites and Sc; (d) 6 cycles of the degradation of MB using sample Sc as the photocatalyst under visible-light irradiation for 30 min.

ZnO/C core-shell nanocables in the degradation of RhB and MB under visible-light irradiation. It is also believed that this synthesis method reported here can be easily extended to prepare a wide variety of functional coaxial nanocables.

Acknowledgements

Financial support from Natural Science Foundation of China (21171146), Zhejiang Provincial Natural Science Foundation of China (Y4110304) and Zhejiang Qianjiang Talent Project (2010R10025) are gratefully acknowledged.

References

1 Y. Z. Fan, M. H. Deng, G. P. Chen, Q. X. Zhang, Y. H. Luo, D. G. Li and Q. B. Meng, *J. Alloys Compd.*, 2011, **509**, 1477.
2 H. Yamashita, M. Harada, J. Misaka, M. Takeuchi, B. Neppolian and M. Anpo, *Catal. Today*, 2003, **84**, 191.
3 B. J. Li and H. Q. Cao, *J. Mater. Chem.*, 2011, **21**, 3346.
4 S. K. Kansal, M. Singh and D. Sudc, *J. Hazard. Mater.*, 2007, **141**, 581.
5 M. R. Hoffmann, S. T. Martin, W. Choi and D. W. Bahnemannt, *Chem. Rev.*, 1995, **95**, 69.
6 Z. Y. Zhang, C. L. Shao, X. H. Li, L. Zhang, H. M. Xue, C. H. Wang and Y. C. Liu, *J. Phys. Chem. C*, 2010, **114**, 7920.
7 N. Kislov, J. Lahiri, H. Verma, D. Y. Goswami, E. Stefanakos and M. Batzill, *Langmuir*, 2009, **25**, 3310.
8 J. L. Yang, S. J. An, W. I. Park, G. C. Yi and W. Choi, *Adv. Mater.*, 2004, **16**, 1661.
9 X. G. Chen, Y. Q. He, Q. Zhang, L. J. Li, D. H. Hu and T. Yin, *J. Mater. Sci.*, 2010, **45**, 953.
10 U. N. Maiti, S. F. Ahmed, M. K. Mitra and K. K. Chattopadhyay, *Mater. Res. Bull.*, 2009, **44**, 134.
11 Y. X. Wang, X. Y. Li, G. Lu, X. Quan and G. H. Chen, *J. Phys. Chem. C*, 2008, **112**, 7332.
12 Y. Hu, H. H. Qian, Y. Liu, G. H. Du, F. M. Zhang, L. B. Wang and X. Hu, *CrystEngComm*, 2011, **13**, 3438.
13 L. W. Zhang, H. Y. Cheng, R. L. Zong and Y. F. Zhu, *J. Phys. Chem. C*, 2009, **113**, 2368.
14 Y. Guo, H. S. Wang, C. L. He, L. J. Qiu and X. B. Cao, *Langmuir*, 2009, **25**, 4678.
15 A. H. Lu, E. L. Salabas and F. Schuth, *Angew. Chem., Int. Ed.*, 2007, **46**, 1222.
16 L. Zhang, W. Z. Wang, M. Shang, S. M. Sun and J. H. Xu, *J. Hazard. Mater.*, 2009, **172**, 1193.
17 Y. Liu, L. Zhou, Y. Hu, C. F. Guo, H. S. Qian, F. M. Zhang and X. W. Lou, *J. Mater. Chem.*, 2011, **21**, 18359.
18 H. W. Liang, W. J. Zhang, Y. N. Ma, X. Cao, Q. F. Guan, W. P. Xu and S. H. Yu, *ACS Nano*, 2011, **5**, 8148.
19 B. Hu, K. Wang, L. H. Wu, S. H. Yu, M. Antonietti and M. M. Titirici, *Adv. Mater.*, 2011, **22**, 813.
20 B. Hu, S. H. Yu, K. Wang, L. Liu and X. W. Xu, *Dalton Trans.*, **2008**, 5414.
21 Y. Liu, Y. Hu, C. F. Guo and X. Hu, *J. Am. Ceram. Soc.*, 2011, **94**, 1667.
22 X. M. Sun and Y. D. Li, *Angew. Chem., Int. Ed.*, 2004, **43**, 597.
23 S. L. Xiong, B. J. Xi and Y. T. Qian, *J. Phys. Chem. C*, 2010, **114**, 14029.
24 A. M. Morales and C. M. Lieber, *Science*, 1998, **279**, 208.
25 G. F. Lin, J. W. Zheng and R. Xu, *J. Phys. Chem. C*, 2008, **112**, 7363.
26 Y. Hu, Y. Liu, H. S. Qian, Z. Q. Li and J. F. Chen, *Langmuir*, 2010, **26**, 18570.
27 Y. Liu, M. J. Zhou, Y. Hu, H. S. Qian, J. F. Chen and X. Hu, *CrystEngComm*, 2012, **14**, 4507.
28 M. Baghbanzadeh, L. Carbone, P. D. Cozzoli and C. O. Kappe, *Angew. Chem., Int. Ed.*, 2011, **50**, 11312.
29 M. S. Raghuveer, S. Agrawal, N. Bishop and G. Ramamath, *Chem. Mater.*, 2006, **18**, 1390.

30 K. Mackenzie, O. Dunens and A. T. Harris, *Sep. Purif. Technol.*, 2009, **66**, 209.
31 L. H. Wu, H. B. Yao, B. Hu and S. H. Yu, *Chem. Mater.*, 2011, **23**, 3946.
32 B. Hu, L. H. Wu, S. J. Liu, H. B. Yao, H. Y. Shi, G. P. Li and S. H. Yu, *Chem. Commun.*, 2010, **46**, 2277.
33 Q. Wang, B. Y. Geng and S. Z. Wang, *Environ. Sci. Technol.*, 2009, **43**, 8968.
34 Y. Y. Li, J. P. Liu, X. T. Huang and J. G. Yu, *Dalton Trans.*, 2010, **39**, 3420.
35 Y. Hu, J. F. Chen, X. Xue, T. W. Li and Y. Xie, *Inorg. Chem.*, 2005, **44**, 7280.
36 S. K. Li, F. Z. Huang, Y. Wang, Y. H. Shen, L. G. Qiu, A. J. Xie and S. J. Xu, *J. Mater. Chem.*, 2011, **21**, 7459.
37 Y. Wang, Y. R. Su, L. Qiao, L. X. Liu, Q. Su, C. Q. Zhu and X. Q. Liu, *Nanotechnology*, 2011, **22**, 225702.